

Magnetic and electronic properties of double-perovskites and estimation of their Curie temperatures by *ab initio* calculations

Tapas Kumar Mandal,¹ Claudia Felser,² Martha Greenblatt,¹ and Jürgen Kübler^{3*}

¹*Department of Chemistry and Chemical Biology, Rutgers,
The State University of New Jersey, 610 Taylor Road, Piscataway, NJ 08854, USA*

²*Institut für Anorganische und Analytische Chemie,
Johannes Gutenberg-Universität, D-55128 Mainz, Germany and*

³*Institut für Festkörperphysik, Technische Universität Darmstadt, D-64289 Darmstadt, Germany**
(Dated: November 1, 2018)

First principles electronic structure calculations have been carried out on ordered double-perovskites $\text{Sr}_2\text{B}'\text{B}''\text{O}_6$ (for $\text{B}' = \text{Cr}$ or Fe and B'' 4d and 5d transition metal elements) with increasing number of valence electrons at the B-sites, and on $\text{Ba}_2\text{MnReO}_6$ as well as $\text{Ba}_2\text{FeMoO}_6$. The Curie temperatures are estimated *ab initio* from the electronic structures obtained with the local spin-density functional approximation, full-potential generalized gradient approximation and/or the LDA+U method (U - Hubbard parameter). Frozen spin-spirals are used to model the excited states needed to evaluate the spherical approximation for the Curie temperatures. In cases, where the induced moments on the oxygen was found to be large, the determination of the Curie temperature is improved by additional exchange functions between the oxygen atoms and between oxygen and B' and B'' atoms. A pronounced systematics can be found among the experimental and/or calculated Curie temperatures and the total valence electrons of the transition metal elements.

PACS numbers: 75.10.Lp, 75.30.Et, 71.20.Be

Keywords: double-perovskites, half-metallic ferroimagnets, electronic structure, Curie temperature

I. INTRODUCTION

Recently, the report of room temperature colossal magnetoresistance (CMR) in the ordered double-perovskite, $\text{Sr}_2\text{FeMoO}_6$ has attracted enormous research interest.¹ The high degree of spin polarization in $\text{Sr}_2\text{FeMoO}_6$ and other magneto resistive materials is believed to be due to the half-metallic nature of these materials.^{1,2,3} Half-metallic materials as proposed by de Groot *et al.*⁴ are metallic with respect to one spin direction whereas the other spin direction is insulating/semiconducting leading to 100 percent spin polarization at the Fermi energy (E_F). At the same time, Kübler *et al.*⁵ also recognized nearly vanishing minority-spin densities at the E_F and suggested about peculiar transport properties in Heusler alloys.

It is known that the giant magnetoresistance GMR can be enhanced in high spin polarized materials. Therefore, materials with a high spin polarization are essential for applications in spintronic devices. Among various families of materials with promising half-metallic ferro/ferrimagnetism (HMF), however, large values of tunnelling magneto resistance (TMR) have not been reported at room temperature, because of their low Curie temperatures (T_C). Thus, finding half-metallic ferromagnetic materials with high T_C is important in the area of spintronics. Some of the double-perovskite oxides have attracted considerable attention due to their very high T_C (well above room temperature).⁶ For example, $\text{Sr}_2\text{CrReO}_6$ is known to be a metallic ferrimagnet with highest T_C of ≈ 635 K. In search of double-perovskites with high T_C , we noticed an intriguing trend (Fig. 1) in the measured T_C s with the total number of

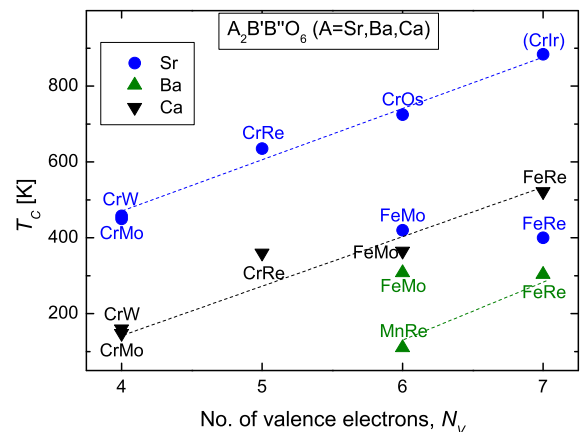


FIG. 1: (Color online) Measured Curie temperatures (T_C) versus the number of valence electrons. The names of the elements $\text{B}'\text{B}''$ in the double-perovskites $\text{A}_2\text{B}'\text{B}''\text{O}_6$ appear near the data points. The value in parenthesis is a projected one.

valence electrons of the transition metals. To emphasize the observed trends we included the Curie temperatures for $\text{Ca}_2\text{B}'\text{B}''\text{O}_6$ which, however, will not be further considered here.

In previous work⁷ the electronic and magnetic structure as well as trends in the Curie temperatures of several Heusler compounds were studied. These are fairly sim-

ple intermetallics for which our theoretical approach was found to work quite well. Chemically completely different are the double-perovskites (intermetallics versus oxides). In contrast to the Heusler compounds the double-perovskites exhibit a larger range of physical properties: not only half-metallic magnets but also magnetic insulators and Mott-Hubbard insulators, for which our theoretical approach is put to a severe test here.

Thus, in this work we have studied the electronic and magnetic structures of several ordered double-perovskites $\text{Sr}_2\text{B}'\text{B}''\text{O}_6$ with $\text{B}' = \text{Cr(III)}$ and Fe(III) while the B'' -site is occupied by a 4d or 5d transition metal element. We also included the interesting pair $\text{Ba}_2\text{MnReO}_6$ and $\text{Ba}_2\text{FeMoO}_6$. A systematic theoretical study of the electronic and magnetic structures of these double-perovskites has been carried out in view of the half-metallic and ferro/ferrimagnetic properties in these materials. The Curie temperatures of known members were calculated *ab initio* to compare with the experimentally measured values. In addition, the calculations have been extended to predict the T_C 's of three new members.

II. COMPUTATIONAL DETAILS

Three different computational procedures were applied to obtain the electronic and magnetic structure of the double-perovskites. The simplest is the local spin-density functional approximation (LSDA) to density functional theory.^{8,9} The numerical work was done using the augmented spherical wave approximation (ASW).¹⁰ In those cases where the magnetic moments of a perovskite under question collapsed in the calculation and/or the expected (see e.g. ref.¹) half-metallic property was not obtained, the LSDA was replaced by a full-potential generalized gradient approximation (GGA).¹¹ Here the numerical work was done with an extension of the ASW-method due to Knöpfle *et al.*¹² In two cases metallic antiferromagnets were obtained in contrast to experimental information.¹³ In this case the electron correlations were assumed to be insufficiently described by both the LSDA and the GGA. Therefore, the semi-empirical LDA+U method¹⁴ was used that is known to provide a relatively simple and good approximation to the problem of correlated electrons. It was incorporated into the ASW-method by Sandratskii.¹⁵ In the present calculations a value for the Hubbard parameter U was employed that is in line with other experience.^{14,16}

The LSDA, the GGA, and LDA+U method, besides serving to describe the electronic structure, are also employed for obtaining low-lying excited states from the total energies of frozen spin-spirals with wave vectors \mathbf{q} , called spiral energies.^{17,18,19} In this context the validity of the adiabatic approximation is tacitly assumed. The spiral energies are expressed as exchange energies or exchange functions, $j_{\tau\tau'}(\mathbf{q})$, which depend on two basis vectors of the constituent magnetic atoms, τ and τ' , and on wave vectors that span the irreducible part of

the Brillouin zone (BZ). The quantities $j_{\tau\tau'}(\mathbf{q})$ are extracted from the spiral energies by an algorithm given in ref.²¹ For the numerical work the force theorem^{22,23} is used, i.e. to obtain the spiral energies the band energies are summed up to the Fermi energy for a given spin configuration using for these calculations the self-consistent ground-state potential.

To estimate the Curie temperatures of the double-perovskites the spherical approximation was used, as described by Moriya²⁴ for itinerant-electron magnetism in elementary systems, and extended to magnetic compounds by one of these authors.²¹ The Curie temperature in this approximation is given by

$$k_B T_c = \frac{2}{3} \sum_{\tau} \mathcal{L}_{\tau}^2 \left[\frac{1}{N} \sum_{\mathbf{q}n} \frac{1}{j_n(\mathbf{q})} \right]^{-1}. \quad (1)$$

Here the exchange functions $j_n(\mathbf{q})$ are eigenvalues of a secular equation and are given in the simplest approximation in terms of three quantities sufficient for the description of the magnetism of double-perovskites, $\text{A}_2\text{B}'\text{B}''\text{O}_6$: $j_{11}(\mathbf{q})$ describing the exchange interaction between the magnetic B' -atoms, $j_{22}(\mathbf{q})$ between the B'' -atoms and $j_{12}(\mathbf{q})$ between the B' - and B'' -atoms. The quantity \mathcal{L}_{τ} in equation (1) is the local moment of the atom at site τ . In principle it must be determined self-consistently, see equation (12) in,²¹ but an acceptable approximation for the double-perovskites is $\mathcal{L}_{\tau} = M_{\tau}$, where M_{τ} is the zero temperature moment of the atom at site τ . This is so, because the magnetic moments are well localized in spite of their originating from itinerant electrons. To support this statement one looks at the change of the local magnetic moments when the tilt of the nearest-neighbor moments is large; in our case the change is less than 0.2 % for the magnetically dominating B' -atoms and round about 1.6 % or less for the weaker moments of the B'' -atoms.

In some of the double-perovskites the induced moments on the oxygen were found to be relatively large, nearly reaching $0.1 \mu_B$ per oxygen, thus adding up to a sizable amount in the unit cell. In these cases the determination of the Curie temperature is improved by using in addition to $j_{11}(\mathbf{q})$, $j_{22}(\mathbf{q})$, and $j_{12}(\mathbf{q})$ three more exchange functions, namely $j_{33}(\mathbf{q})$, $j_{13}(\mathbf{q})$, and $j_{23}(\mathbf{q})$ that describe the interaction between the O-atoms, between the O-atoms and atom B' , and the O-atoms and atom B'' , respectively. These parameters are also extracted from the spiral energies in a somewhat cumbersome procedure. The details are omitted here.

III. RESULTS OF THE CALCULATIONS

In presenting the results of our calculations we use as a "coordinate" the number of total valence electrons, N_V , in the double-perovskite, $\text{A}_2\text{B}'\text{B}''\text{O}_6$, that are supplied by the transition metal elements B' and B'' . The remaining electrons from the A- and O-atoms remain the same in

TABLE I: Collection of pertinent experimental and calculated data for 12 double-perovskites, $\text{Sr}_2\text{B}'\text{B}''\text{O}_6$ and for $\text{Ba}_2\text{MnReO}_6$ as well as $\text{Ba}_2\text{FeMoO}_6$. The quantity N_V is the total number of valence electrons supplied by B' and B'' . The space group symmetry is given in the column, *symm.*, where known. The type of the calculated magnetic structure is given in the column, *type*, where HMF stands for half-metallic ferrimagnet, MIN for magnetic insulator, and MHI for Mott-Hubbard insulator. The total calculated magnetic moment, $M_{\text{tot}}^{\text{calc}}$ is given in μ_B per formula unit. The local moment of B' is denoted by $\mathcal{L}_{\text{B}'}$, that of B'' by $\mathcal{L}_{\text{B}''}$, and the induced moments of the 6 O atoms by $6\mathcal{L}_O$, all in units of μ_B . The calculated Curie temperatures, T_C^{calc} , and the experimental ones, T_C^{exp} , are given in K.

Compound	N_V	<i>symm.</i>	$a[\text{\AA}]$	<i>type</i>	$M_{\text{tot}}^{\text{calc}}$	$\mathcal{L}_{\text{B}'}$	$\mathcal{L}_{\text{B}''}$	$6\mathcal{L}_O$	T_C^{calc}	$T_C^{\text{exp}(b)}$
$\text{Sr}_2\text{CrMoO}_6$	4	$Fm\bar{3}m^{(a)}$	$7.840^{(a)}$	HMF ⁽¹⁾	2.0	2.251	-0.357	0.106	379	420
Sr_2CrWO_6	4	$Fm\bar{3}m^{(b)}$	$7.832^{(b)}$	HMF ⁽²⁾	2.0	2.557	-0.439	0.082	434	458
$\text{Sr}_2\text{CrReO}_6$	5	$I4/m^{(c)}$	$7.814^{(c,d)}$	HMF ⁽²⁾	1.0	2.423	-1.272	-0.151	742	620
$\text{Sr}_2\text{CrRuO}_6$	6	$Fm\bar{3}m^{(e)}$	$7.903^{(e)}$	MIN ⁽¹⁾	0.0	2.222	-1.718	-0.504	577 ⁽⁴⁾	
$\text{Sr}_2\text{CrOsO}_6$	6	$Fm\bar{3}m^{(f)}$	$7.824^{(f)}$	MIN ⁽²⁾	0.0	2.443	-1.893	-0.550	881	725
$\text{Sr}_2\text{CrIrO}_6$	7	$Fm\bar{3}m^{(e)}$	$7.881^{(e)}$	HMF ⁽²⁾	1.0	2.296	-0.953	-0.343	884	
$\text{Sr}_2\text{FeMoO}_6$	6	$I4/m^{(b)}$	$7.894^{(b,d)}$	HMF ⁽¹⁾	4.0	3.792	-0.355	0.563	360	420
$\text{Sr}_2\text{FeTcO}_6$	7	$Fm\bar{3}m^{(e)}$	$7.919^{(e)}$	HMF ⁽¹⁾	2.99	3.665	-1.087	0.415	160	
$\text{Sr}_2\text{FeReO}_6$	7	$I4/m^{(b)}$	$7.877^{(b,d)}$	HMF ⁽¹⁾	3.0	3.763	-1.028	0.265	384	400
$\text{Sr}_2\text{FeRuO}_6$	8	$Fm\bar{3}m^{(e)}$	$7.919^{(e)}$	MHI ⁽³⁾	0.0	3.613	1.912 ⁽⁵⁾	0.02		
$\text{Ba}_2\text{FeMoO}_6$	6	$Fm\bar{3}mm^{(b)}$	$8.012\text{m}^{(b)}$	HMF ⁽¹⁾	4.0	3.564	-0.215	0.651	331 ⁽⁴⁾	308
$\text{Ba}_2\text{MnReO}_6$	6	$Fm\bar{3}mm^{(b)}$	$8.186\text{m}^{(b)}$	HMF ⁽³⁾	4.0	4.234	-0.622	0.388	71 ⁽³⁾	110

⁽¹⁾From LSDA calculation. ⁽²⁾From GGA calculation. ⁽³⁾From LDA+U calculation.

⁽⁴⁾Obtained with 6 exchange functions. ⁽⁵⁾Orthogonal to B' -moment.

^(a)From Arulraj *et al.*²⁵ ^(b)From Serrate *et al.*⁶ ^(c)From Kato *et al.*²⁶

^(d)Calculated from experimental atomic volume. ^(e)Assumed values. ^(f)From Krockenberger *et al.*²⁷

the series under investigation, which leads us to suppress them in the presentation. However, we will notice that chemical valence will not obey such a simple scheme.

We begin with Table I and the Figs. 2, 3 and 4. The measured crystal structures and lattice constants given in Table I were used in the calculations except when they are tetragonal ($I4/m$). In these cases the crystal structure was approximated by a cubic cell ($Fm\bar{3}m$) using lattice constants that were calculated from the measured atomic volumes. It is seen that for the first five compounds, $\text{Sr}_2\text{CrB}''\text{O}_6$ with $\text{B}'' = \text{Mo}, \text{W}, \text{Re}, \text{Ru}, \text{and Os}$, N_V increases ($N_V = 4, 5$ and 6), whereas the calculated total magnetic moments, $M_{\text{tot}}^{\text{calc}}$ decrease. This is so, because the individual moments of Cr and B'' couple antiparallel until they are entirely compensated for the compounds $\text{Sr}_2\text{CrRuO}_6$ and $\text{Sr}_2\text{CrOsO}_6$. The latter could thus be called zero-moment ferrimagnets. The densities of states (DOS) shown in Fig. 2 and 3 ($\text{Sr}_2\text{CrMoO}_6$, Sr_2CrWO_6 and $\text{Sr}_2\text{CrReO}_6$) show a gap at the Fermi energy in the up-spin direction (upper parts of the graphs) typical for half-metallic ferrimagnetism (HMF). In all the DOS figures the energy is counted from the Fermi energy.

The dominant structures at low energies (black lines) are mainly due to the O 2*p*-electrons. For $\text{Sr}_2\text{CrRuO}_6$ and $\text{Sr}_2\text{CrOsO}_6$ shown in Fig. 4 the half-metallic gap is found in the down-spin electrons. $\text{Sr}_2\text{CrOsO}_6$ has been made by Krockenberger *et al.*,²⁷ who also computed the electronic structure, which is in agreement with Fig. 4 as far as the insulating property is concerned.

Also insulating with zero gap in the up-spin electrons is the compound $\text{Sr}_2\text{CrRuO}_6$, shown in Fig. 4. In Table I the label MIN is understood to mean magnetic insulator. Clearly, it is of a different kind than for instance NiO, which is known to be a Mott-Hubbard insulator. A recent calculation by Lee and Pickett²⁸ agrees fairly well with ours. Our attempts to prepare this phase under ambient pressure have not been successful thus far. The Curie temperature is predicted to be 577 K in the approximation with 6 exchange functions. A larger value of 719 K is obtained in the simpler approximation with 3 exchange functions, where the induced magnetic moments of oxygen are ignored. The latter value, although less reliable, seems to conform more with the trend shown in Fig. 1 than the former.

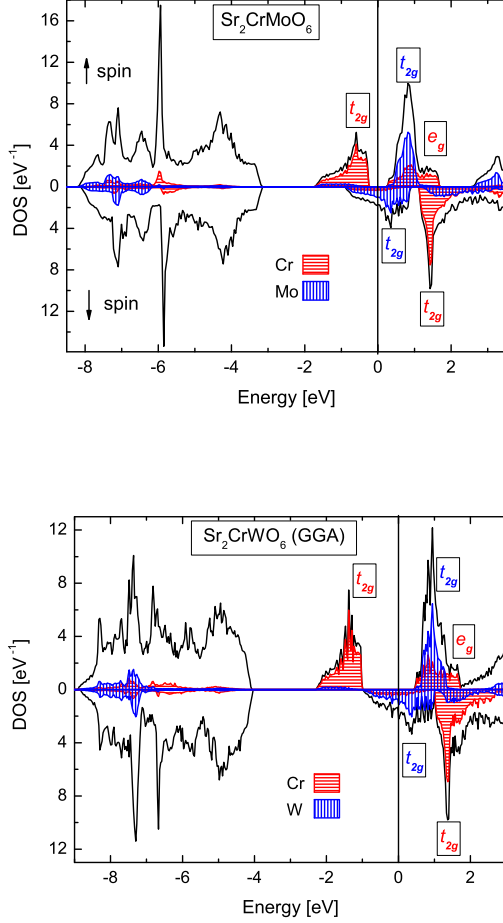


FIG. 2: (Color online) Total (black) and partial (colored) density of states of $\text{Sr}_2\text{CrMoO}_6$ and Sr_2CrWO_6 . The total number of valence electrons from Cr(III) and Mo(V) is $N_V = 4$, same for Cr and W. The total magnetic moment is in each case $M_{\text{tot}} = 2.0 \mu_B$ per formula unit (f.u.). Symmetry labels of the parent states are included.

Our electronic structure calculation of $\text{Sr}_2\text{CrReO}_6$ in absence of spin-orbit coupling resulted a total magnetic moment of $1.0 \mu_B$ per formula unit and a half-metallic ferrimagnetic (HMF) ground state. However, recently it has been shown experimentally that the system is not half-metallic, in the true sense, due to a large orbital contribution to the magnetization (saturation was obtained only at a much higher field, ≈ 20 T).^{29,30} The measured saturation magnetization of $1.38 \mu_B$ for $\text{Sr}_2\text{CrReO}_6$ was close to the value theoretically predicted by Vaitheeswaran *et al.*³¹

The next member in the series with $N_V = 7$, $\text{Sr}_2\text{CrIrO}_6$, is an interesting case. A calculation of the electronic structure using the GGA gives a half-metallic ferrimagnet, for which the density of states is shown in

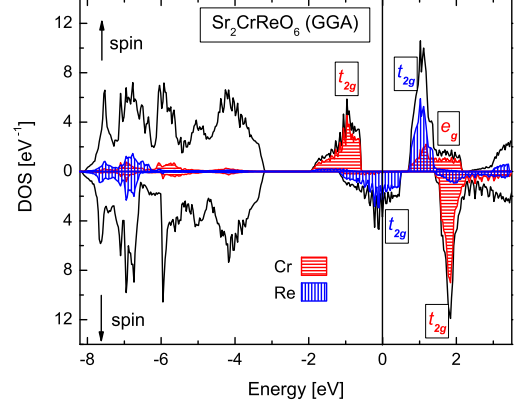


FIG. 3: (Color online) Total (black) and partial (colored) density of states of $\text{Sr}_2\text{CrReO}_6$. The number of valence electrons from Cr(III) and Re(V) is $N_V = 5$. The total magnetic moment is $M_{\text{tot}} = 1.0 \mu_B$ per f.u. Symmetry labels of the parent states are included.

Fig. 5. A calculation of the Curie temperature results in $T_C = 884$ K which is used as the projected value in Fig. 1. However, this HMF-state is most likely metastable because a total-energy search returns a metallic antiferromagnet of the AFII structure, which corresponds in a k-vector notation to $\mathbf{K} = (\frac{1}{2}, \frac{1}{2}, \frac{1}{2})$. In this configuration the magnetic moments are aligned ferromagnetically in the (111) plane and alternate along the [111] direction. This result has to be questioned: correlations are likely to alter the electronic structure and result in a Mott-Hubbard insulator. LDA+U calculations were therefore employed but we find that even in this case the antiferromagnet remains metallic. Comparable calculations by Fang *et al.*¹⁶ also show that the LDA+U method not always opens a gap at the Fermi energy.

In calculating the Curie temperature by means of equation (1) the eigenvalues $j_n(\mathbf{q})$ are approximations of the spin-wave spectrum. Negative values of $j_n(\mathbf{q})$ are unphysical and usually signal that the assumed magnetic structure is incorrect. Since this was not seen in the present calculations for the HMF-state, we conclude that this state is at least metastable. Furthermore, the spin-wave spectrum for the metallic antiferromagnet obtained by means of the LDA+U method is found to be unphysical. Thus we discard the antiferromagnetic solution but cannot predict that experimentally prepared $\text{Sr}_2\text{CrIrO}_6$ will be a HMF.

Next we concentrate on the Fe containing double-perovskites, $\text{Sr}_2\text{FeB''O}_6$ with increasing number of valence electrons on the transition metal atoms (Table I). For the $N_V = 6$ - double-perovskite, $\text{Sr}_2\text{FeMoO}_6$, we show the densities of states in Fig. 6. We see HMF behavior with a large total magnetic moment of $M_{\text{tot}} = 4 \mu_B$ per

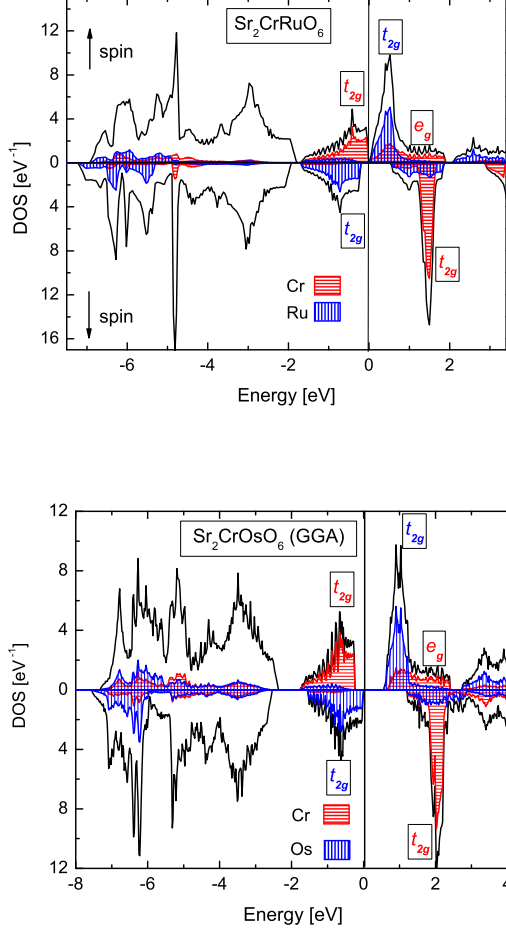


FIG. 4: (Color online) Total (black) and partial (colored) density of states of $\text{Sr}_2\text{CrRuO}_6$ and $\text{Sr}_2\text{CrOsO}_6$. The number of valence electrons from Cr(III) and Ru(V) is $N_V = 6$, same for Cr and Os. The total magnetic moment in each case compensates to $M_{\text{tot}} = 0.0 \mu_B$ per f.u. Symmetry labels of the parent states are included.

f.u. The DOS for $\text{Sr}_2\text{FeMoO}_6$ is nearly identical with that previously obtained by Kobayashi *et al.*¹ and Fang *et al.*¹⁶ Another earlier study by Sarma *et al.*³² also agrees with our calculations. In this case, our calculation for the Curie temperature underestimates the experimental value and gives 360 K, which is to be compared with the experimental value of 420 K. The LSDA was used here for simplicity, although the GGA might result in a somewhat better estimate.

The double-perovskite series for $B' = \text{Fe}$ and $N_V = 7$, we continue with $\text{Sr}_2\text{FeTcO}_6$ and $\text{Sr}_2\text{FeReO}_6$ for which the densities of states are shown in Fig. 7. Both are HMF. For $\text{Sr}_2\text{FeTcO}_6$ the Curie temperature we calculate to be about 160 K, which is most likely underestimated. $\text{Sr}_2\text{FeReO}_6$ possesses a total magnetic moment of

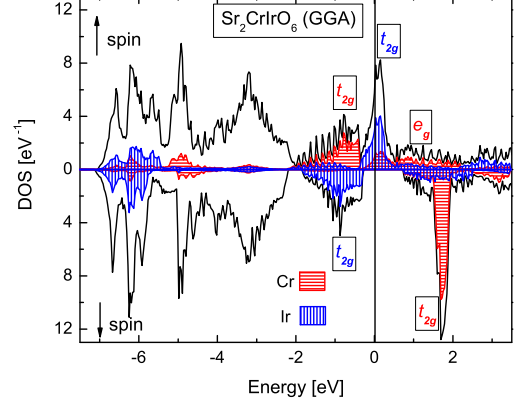


FIG. 5: (Color online) Total (black) and partial (colored) density of states of $\text{Sr}_2\text{CrIrO}_6$. The number of valence electrons from Cr(III) and Ir(V) is $N_V = 7$. The total magnetic moment is $M = 1 \mu_B$ p.f.u. Symmetry labels of the parent states are included.

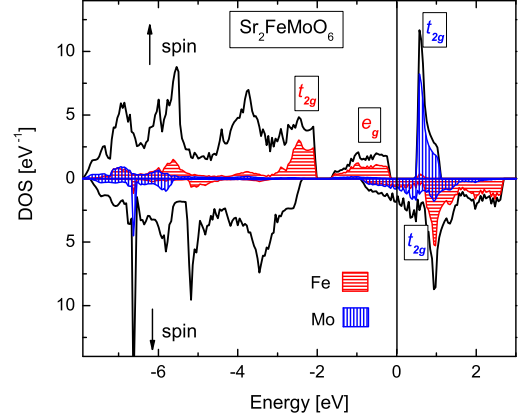


FIG. 6: (Color online) Total (black) and partial (colored) density of states of $\text{Sr}_2\text{FeMoO}_6$. The number of valence electrons from Fe(III) and Mo(V) is $N_V = 6$. The total magnetic moment is $M_{\text{tot}} = 4.0 \mu_B$ per f.u. Symmetry labels of the parent states are included.

$M_{\text{tot}} = 3 \mu_B$, which is the result of a ferrimagnetic moment arrangement comparable to the $N_V = 4$ to 6 cases in $\text{Sr}_2\text{CrB}''\text{O}_6$ series. The DOS for $\text{Sr}_2\text{FeReO}_6$ shown in Fig. 7 is nearly identical with the previously published results by Fang *et al.*¹⁶ Our calculation for the Curie temperature gives $T_C = 384$ K in good agreement with the measured value of 400 K. We remark that the calculations were done using an idealized cubic structure and the simple LSDA.

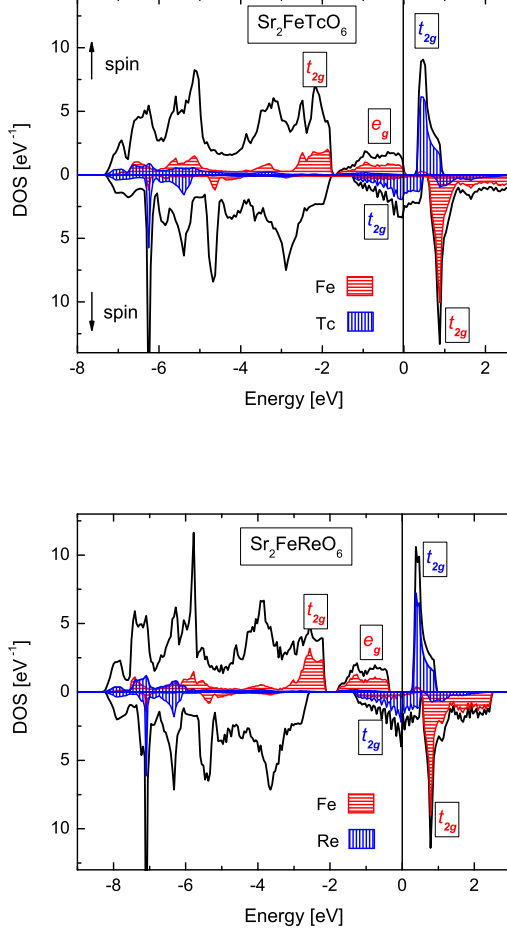


FIG. 7: (Color online) Total (black) and partial (colored) density of states of $\text{Sr}_2\text{FeTcO}_6$ and $\text{Sr}_2\text{FeReO}_6$. The number of valence electrons from Fe(III) and Tc(V) is $N_V = 7$, same for Fe and Re. The total magnetic moment is $M_{\text{tot}} = 3.0 \mu_B$ per f.u. and nearly so for $\text{Sr}_2\text{FeTcO}_6$. Symmetry labels of the parent states are included.

The case of $N_V = 8$, $\text{Sr}_2\text{FeRuO}_6$, is again found to be unstable as a ferromagnet with an unphysical spin-wave spectrum (SWS). This means a branch of the SWS becomes negative indicating that the assumed state is not the ground state. A search for the correct state was carried out via the non-collinear states formed by spin-spirals which lead to a total-energy minimum at $\mathbf{K} = (\frac{1}{2}, \frac{1}{2}, \frac{1}{2})$. This is again the AFII structure; it is metallic. As in the previous case for $\text{Sr}_2\text{CrIrO}_6$, the metallic antiferromagnetic solution found here has to be questioned. Thus, taking into account electron correlations again by the LDA+U method we find $\text{Sr}_2\text{FeRuO}_6$ to be a Mott-Hubbart insulator (MHI) with a small gap at the Fermi energy, see Fig. 8. Here the two Fe-peaks below -6 eV are the filled t_{2g} - and e_g -states pushed to

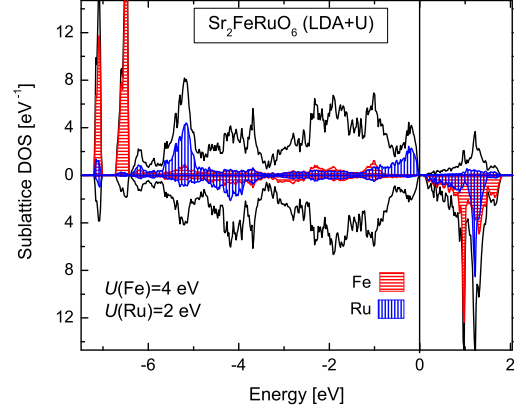


FIG. 8: (Color online) Total (black) and sublattice density of states of antiferromagnetic (AFII or $\mathbf{K} = (0.5, 0.5, 0.5)$) $\text{Sr}_2\text{FeRuO}_6$. LDA+U was used. The number of valence electrons from Fe(III) and Ru(V) is $N_V = 8$.

this low energy by the Hubbard U . In contrast to the observations of Fang *et al.*,¹⁶ we find the magnetic moment of Ru to be stable and arranged orthogonal to the Fe moments. However, an attempt to determine the Néel temperature failed because the SWS dipped into unphysical negative values again. Thus the MHI as determined here still has to be questioned.

We finish with two double-perovskites having $N_V = 6$: $\text{Ba}_2\text{FeMoO}_6$ and $\text{Ba}_2\text{MnReO}_6$. Although somewhat outside the series discussed above, we find them of importance for supporting the predictive nature of our calculations.

Fig. 9 shows that $\text{Ba}_2\text{FeMoO}_6$ is a HMF. Because of the relatively large induced oxygen moments (see Table I) we use six exchange functions and calculate the Curie temperature to be $T_C = 331$ K, which is to be compared with the measured value of 308 K. In contrast to this rather straight-forward LSDA-calculation is the case of $\text{Ba}_2\text{MnReO}_6$.

In both the LSDA and the GGA the electronic structure is calculated to be a metallic ferrimagnet with spin-up Mn- t_{2g} -states and spin-down Re- e_g -states at the Fermi energy. This is in stark contrast to measurements by Popov *et al.*¹³ who found this compound to be of high resistivity. We therefore applied the LDA+U method and obtain a HMF. The DOS is shown in the lower portion of Fig. 9. Comparing with the case of $\text{Ba}_2\text{FeMoO}_6$ in the upper portion of the Fig. 9 we see that all spin-up Mn states are well below E_F and the states at E_F are almost purely spin-down Re states. The calculated Curie temperature is 71 K which is in fair agreement with the measured value of 110 K.

In Fig. 10 we finally compare all measured and calculated Curie temperatures.

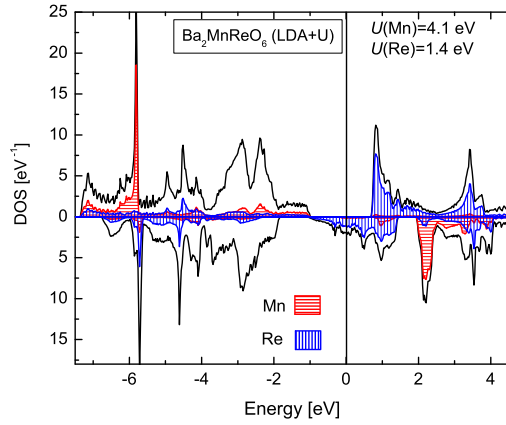
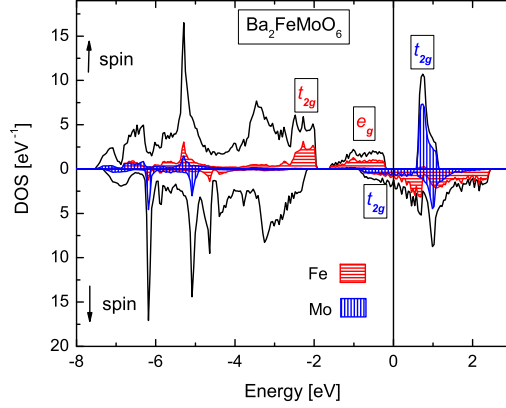


FIG. 9: (Color online) Total (black) and partial (colored) density of states of $\text{Ba}_2\text{FeMoO}_6$ and $\text{Ba}_2\text{MnReO}_6$. The number of conduction electrons from Fe and Mo (Mn and Re) is $N_V=6$. The total magnetic moment is $M_{\text{tot}} = 4.0 \mu_B$ per f.u. The LDA+U method was employed in the case of $\text{Ba}_2\text{MnReO}_6$.

IV. SUMMARY

An overall view of the electronic and magnetic structure of the two series considered here is easily obtained by using the simplified level scheme graphed in Fig. 11, which takes into account the crystal-field splitting of an octahedral environment, viz. t_{2g} and e_g .

Since the two transition metals are coupled antiferromagnetically the double-perovskites can be half metallic ferrimagnets (HMF), antiferromagnets or magnetic insulators (MIN), depending on the valence electron count. The single exception is $\text{Sr}_2\text{CrIrO}_6$, where the magnetic interaction is more complex. Comparing with Figs. 2 and 3, we see that Fig. 11 (a) captures the physics well. When the cations both have a spin configuration of d^3 the compound becomes a MIN, as is the case for $\text{Sr}_2\text{CrOsO}_6$

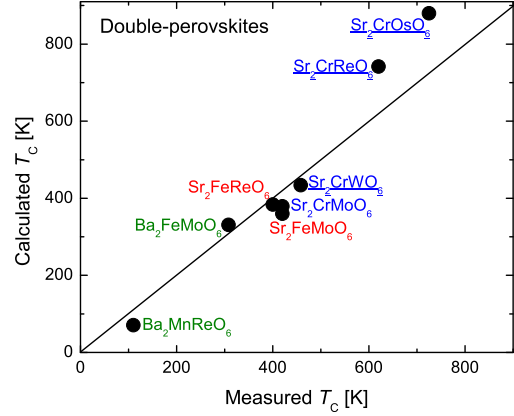


FIG. 10: (Color online) Calculated versus measured Curie temperatures. Underlined: GGA was used; for $\text{Ba}_2\text{MnReO}_6$ LDA+U was used.

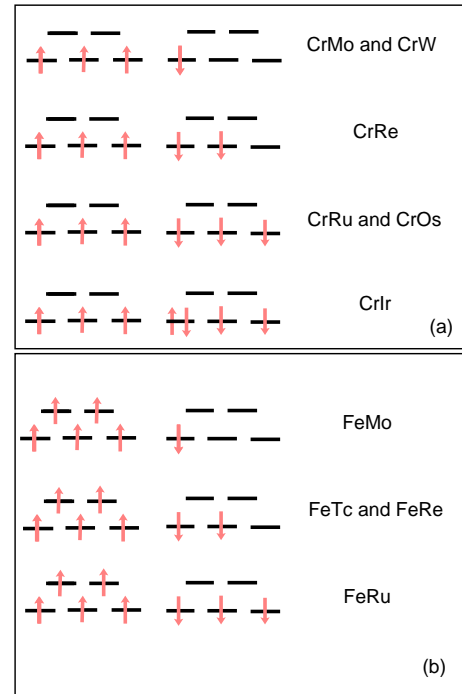


FIG. 11: (Color online) Schematic level diagram for (a) the series $\text{Sr}_2\text{CrB}''\text{O}_6$ and (b) $\text{Sr}_2\text{FeB}''\text{O}_6$. Three lines symbolize the t_{2g} -states and two the e_g -states. The number of valence electrons, N_V , is given by the sum of the arrows, which (by our definition used in Figs. 2 to 9) count the up- and down-spin occupations.

and $\text{Sr}_2\text{CrRuO}_6$ shown in Fig. 4. The series represented by Fig. 11 (b) is terminated by the Mott-Hubbard insulator $\text{Sr}_2\text{FeRuO}_6$ where the cations have the spin configuration d^5 and d^3 . The two double-perovskites $\text{Ba}_2\text{FeMoO}_6$ and $\text{Ba}_2\text{MnReO}_6$ shown in Fig. 9 are represented in Fig. 11 (b) by the FeMo entry.

Our *ab initio* calculations of the Curie temperatures of the double-perovskites reproduced the trend shown in Fig. 1 even though we simplified the crystal structure by using cubic cells. The spherical approximation together with the use of spin-spirals proved to be quite reliable here. A glance at Fig. 10 reveals deviations especially in the calculations where the GGA had to be used. It is emphasized, however, that the neglected structural distortions and anti-site disorder can influence the measured magnetic properties so that a comparison with the idealized calculations may only result in qualitative understanding.

Finally, the large Curie temperatures, especially for $\text{Sr}_2\text{CrReO}_6$ and $\text{Sr}_2\text{CrOsO}_6$, require remarkably large ferromagnetic exchange interactions between the Cr cations. This issue was raised by Sarma *et al.*³² and in large detail by Fang *et al.*¹⁶ who invoked a mechanism that is

comparable to double exchange (DE).^{33,34} This mechanism involves charge carriers and is thus operative for the half metallic ferrimagnets. For the magnetic insulators $\text{Sr}_2\text{CrOsO}_6$ and $\text{Sr}_2\text{CrRuO}_6$ and the Mott-Hubbard insulator $\text{Sr}_2\text{FeRuO}_6$ we resort to the antiferromagnetic superexchange (SE),³⁵ which through the $4d$ - and $5d$ -cations results in ferromagnetic exchange between the $3d$ -cations. The interaction path that is typical for both DE and SE possesses a distinctly visible fingerprint in the Figs. 2 to 9 where the oxygen-transition-metal hybridization is clearly visible at an energy of about -7 eV to -6 eV.

Acknowledgments

J.K. is grateful to L.M. Sandratskii for letting him use his LDA+U code. T.K.M. and M.G. thank the National Science Foundation for financial support through NSF-DMR-0233697 and NSF-DMR-0541911. C.F. and J.K. acknowledge the financial support by the Deutsche Forschungsgemeinschaft in research unit FG 559.

* Electronic address: jkubler@fkp.tu-darmstadt.de

- ¹ K.-I. Kobayashi, T. Kimura, H. Sawada, K. Terakura, and Y. Tokura, *Nature* **395**, 677 (1998).
- ² Y. Okimoto, T. Katsufuji, T. Ishikawa, A. Urushibara, T. Arima, and Y. Tokura, *Phys. Rev. Lett.* **75**, 109 (1995).
- ³ J. H. Park, E. Vescovo, H. J. Kim, C. Kwon, R. Ramesh, and T. Venkatesan, *Nature* **392**, 794 (1998).
- ⁴ R. A. de Groot, F. M. Mueller, P. G. van Engen, and K. H. J. Buschow, *Phys. Rev. Lett.* **50**, 2024 (1983).
- ⁵ J. Kübler, A. R. Williams, and C. B. Sommers, *Phys. Rev. B* **28**, 1745 (1983).
- ⁶ D. Serrate, J. M. De Teresa, and M. R. Ibarra, *J. Phys. CM: Condens. Matter* **19**, 023201 (2007).
- ⁷ J. Kübler, G. H. Fecher, and C. Felser, *Phys. Rev. B* **76**, 024414 (2007).
- ⁸ W. Kohn and L. J. Sham, *Phys. Rev.* **140**, A1133 (1965).
- ⁹ U. von Barth and L. Hedin, *J. Phys. C: Sol. State Phys.* **5**, 1629 (1972).
- ¹⁰ A. R. Williams, J. Kübler, and C. D. Gelatt, *Phys. Rev. B* **19**, 6094 (1979).
- ¹¹ J. P. Perdew, K. Burke, and M. Ernzerhof, *Phys. Rev. Lett.* **77**, 3865 (1996).
- ¹² K. Knöpfle, L. M. Sandratskii, and J. Kübler, *Phys. Rev. B* **62**, 5564 (2000).
- ¹³ G. Popov, M. Greenblatt, M. Croft, *Phys. Rev. B* **67**, 024406 (2003).
- ¹⁴ V. I. Anisimov, J. Zaanen, and O. K. Andersen, *Phys. Rev. B* **44**, 943 (1991).
- ¹⁵ L. M. Sandratskii, unpublished (2006).
- ¹⁶ Z. Fang, K. Terakura, and J. Kanamori, *Phys. Rev. B* **63**, 180407(R) (2001).
- ¹⁷ C. Herrington, in *Magnetism IV*, edited by G. Rado and H. Suhl (Academic Press, New York, 1966).

- ¹⁸ L. M. Sandratskii, *J. Phys. F: Metal Phys.* **16**, L43 (1986).
- ¹⁹ L. M. Sandratskii, *Adv. Phys.* **47**, 91 (1998).
- ²⁰ G. Popov, V. Lobanov, E.V. Tsiper, M. Greenblatt, E.N. Caspi, A. Borissov, V. Kiryukhin, and J.W. Lynn, *J. Phys.: Condens. Matter* **16**, 135 (2004).
- ²¹ J. Kübler, *J. Phys.: Condens. Matter* **18**, 9795 (2006).
- ²² V. Heine, in *Solid State Physics*, edited by H. Ehrenreich, F. Seitz, and P. Turnbull (Academic Press, New York, 1980), vol. 35.
- ²³ A. R. Mackintosh and O. K. Andersen, in *Electrons at the Fermi surface*, edited by S. M. (Cambridge University Press, Cambridge, 1980).
- ²⁴ T. Moriya, *Spin Fluctuations in Itinerant Electron Magnetism* (Springer Verlag, Berlin, 1985).
- ²⁵ A. Arulraj, K. Ramesha, J. Gopalakrishnan, and C.N.N. Rao, *J. Sol. State Chem.* **155**, 233 (2000).
- ²⁶ H. Kato, T. Okuda, Y. Okimoto, Y. Tomioka, K. Oikawa, T. Kamiyama, and Y. Tokura, *Phys. Rev. B* **69**, 184412 (2004).
- ²⁷ Y. Krockenberger, K. Mogare, M. Reehuis, M. Tovar, M. Jansen, G. Vaitheeswaran, V. Kanchana, F. Bultmark, A. Delin, F. Wilhelm, A. Rogalev, A. Winkler, and L. Alff, *Phys. Rev. B* **75**, 020404(R) (2007).
- ²⁸ K.-W. Lee and W. E. Pickett, *Phys. Rev. B* **77**, 115101 (2008).
- ²⁹ J. M. Michalik, J. M. De Teresa, C. Ritter, J. Blasco, D. Serrate, M. R. Ibarra, C. Kapusta, J. Freudenberger, and N. Kozlova, *Europhys. Lett.* **78**, 17006 (2007).
- ³⁰ J. M. De Teresa, J. M. Michalik, J. Blasco, P. A. Algarabel, M. R. Ibarra, C. Kapusta, and U. Zeitler, *Appl. Phys. Lett.* **90**, 252514 (2007).
- ³¹ G. Vaitheeswaran, V. Kanchana, and A. Delin, *Appl. Phys. Lett.* **86**, 032513 (2005).
- ³² D. D. Sarma, P. Mahadevan, T. S. Dasgupta, S. Ray,

- and A. Kumar, Phys. Rev. Lett. **85**, 2549 (2000).
- ³³ P. W. Anderson, and H. Hasegawa, Phys. Rev. **100**, 675 (1955).
- ³⁴ P.-G. de Gennes, Phys. Rev. **118**, 141 (1960).
- ³⁵ P. W. Anderson, Phys. Rev. **79**, 350 (1950).